JACS
JOURNAL OF THE AMERICAN CHEMICAL SOCIETY

Article

pubs.acs.org/JACS

Functional Modulation of a G Protein-Coupled Receptor Conformational Landscape in a Lipid Bilayer

Marina Casiraghi,[†] Marjorie Damian,[‡] Ewen Lescop,[§] Elodie Point,[†] Karine Moncoq,[†] Nelly Morellet,[§] Daniel Levy,[∥,⊥,#] Jacky Marie,[‡] Eric Guittet,[§] Jean-Louis Banères,[*,‡] and Laurent J. Catoire[*,†]

[†]Laboratoire de Biologie Physico-Chimique des Protéines Membranaires, UMR 7099, CNRS/Université Paris Diderot, Sorbonne Paris Cité, Institut de Biologie Physico-Chimique (FRC 550), 13 rue Pierre et Marie Curie, F-75005 Paris, France

[‡]Institut des Biomolécules Max Mousseron (IBMM), UMR 5247 CNRS-Université Montpellier-ENSCM, Faculté de Pharmacie, 15 Avenue C. Flahault, F-34093 Montpellier, France

[§]Institut de Chimie des Substances Naturelles, CNRS UPR 2301, Université Paris-Sud, 91198 Gif-sur-Yvette, France

[∥]Institut Curie, Centre de Recherche, 75231 Paris, France

[⊥]UMR 168, CNRS, 75231 Paris, France

[#]Université Pierre et Marie Curie, F-75248 Paris, France

Supporting Information

ABSTRACT: Mapping the conformational landscape of G protein-coupled receptors (GPCRs), and in particular how this landscape is modulated by the membrane environment, is required to gain a clear picture of how signaling proceeds. To this end, we have developed an original strategy based on solution-state nuclear magnetic resonance combined with an efficient isotope labeling scheme. This strategy was applied to a typical GPCR, the leukotriene B_4 receptor BLT2, reconstituted in a lipid bilayer. Because of this, we are able to provide direct evidence that BLT2 explores a complex landscape that includes four different conformational states for the unliganded receptor. The relative distribution of the different states is modulated by ligands and the sterol content of the membrane, in parallel with the changes in the ability of the receptor to activate its cognate G protein. This demonstrates a conformational coupling between the agonist and the membrane environment that is likely to be fundamental for GPCR signaling.

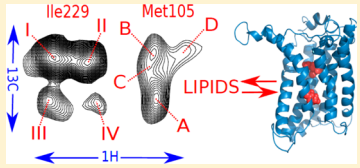

INTRODUCTION

Deciphering the mechanism of signal transduction through G protein-coupled receptors (GPCRs) is a major issue in biology and the subject of intense research.[1] The conformational dynamics of GPCRs is central to their signaling plasticity and allosteric regulation[2] but still poorly delineated. In particular, the impact of the membrane environment is barely understood, although it has been repeatedly demonstrated that it plays a central role in membrane protein structure and dynamics.[3] Additional biophysical studies besides existing crystallographic analyses are thus required to complete the description of the conformational space of GPCRs and how it can be modulated by ligands, signaling proteins, and membrane composition.

In this context, solution-state nuclear magnetic resonance (NMR) spectroscopy appears as a promising method as it can provide dynamic pictures of molecules at physiological temperatures at the atomic scale over a time scale of picoseconds to seconds and beyond.[4,5] So far, NMR studies of GPCR conformational exchange have been performed for only a very limited number of receptors.[6−14] Most of these studies were nevertheless conducted in detergent solutions. Detergents can affect the stability of isolated receptors[15] and have an impact on their conformational equilibrium through a fast chemical exchange at the surface of the protein.[16] This also precludes a detailed analysis of the influence of the membrane structure on receptor dynamics. Among all these studies, only one was performed with a receptor in nanodiscs,[13] but in this case, the β_2-adrenergic receptor was only partially deuterated, dramatically affecting spectral resolution. Indeed, all the NMR studies relied on either protonated or fluorinated methyl groups within fully protonated proteins[6−12] or a partially and inhomogeneously deuterated receptor.[13] However, the impact of modified residues or fluorinated probes on the protein conformational exchange is difficult to gauge. This can be particularly true near binding sites and/or at sites where conformational changes are likely to occur and where probes are usually located for optimal sensitivity to interaction and/or activation. Finally, well-resolved NMR data can be obtained with protonated seven-transmembrane helix proteins provided these proteins are rigid, either naturally[17] or because of thermostabilizing mutations.[14] In all other cases, with unmodified proteins, the NMR signals were very broad because of a residual or fully protonated dipolar environment so that detection of subtle differences in chemical shifts was impossible. This arises because even a residual amount of protons can dramatically affect the relaxation properties of the nuclei under investigation. This is particularly important for the large, slow-

Received: May 6, 2016
Published: August 4, 2016

DOI: 10.1021/jacs.6b04432
J. Am. Chem. Soc. 2016, 138, 11170−11175

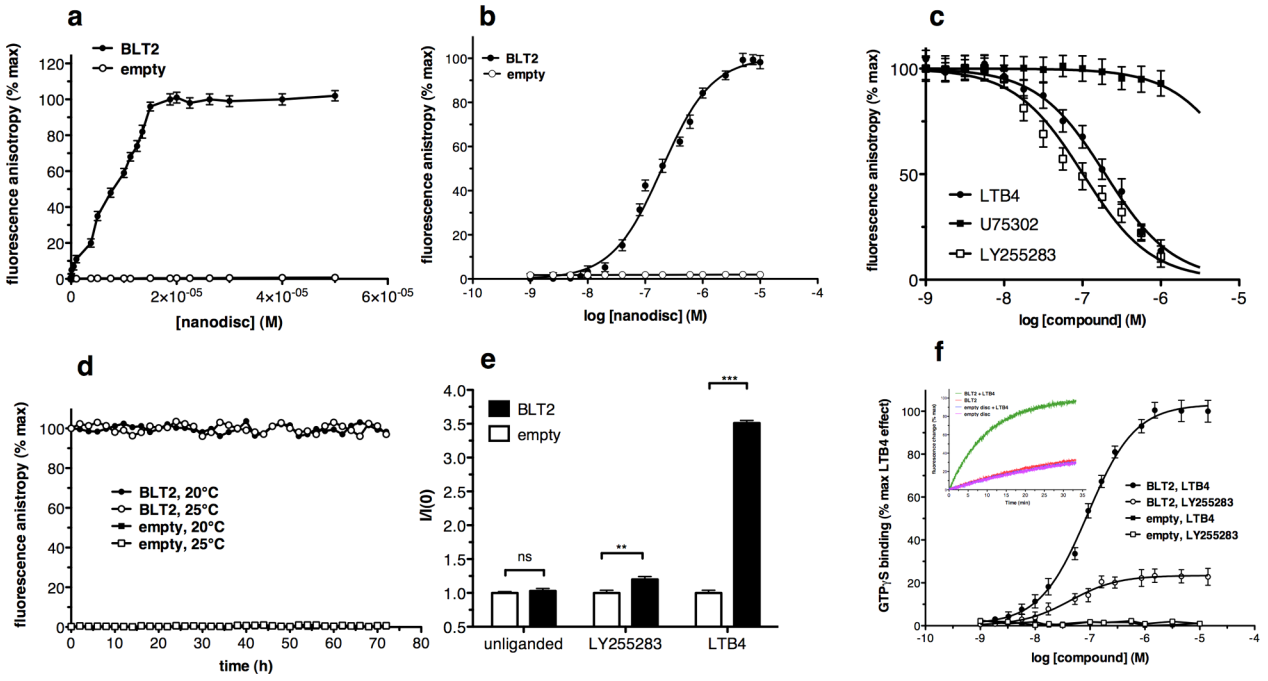

Figure 1. Pharmacology of BLT2 in nanodiscs. (a) Fluorescence anisotropy-monitored stoichiometric titration of LTB4-568 by BLT2-containing nanodiscs (●) or empty nanodiscs (○). (b) Fluorescence anisotropy-monitored dose-response binding of LTB4-568 to BLT2-containing nanodiscs (●) or empty nanodiscs (○). (c) Competitive binding data for inhibition of binding of LTB4-568 to BLT2-containing nanodiscs in the presence of a leukotriene B4 receptor ligand. (d) Variations in the fluorescence anisotropy signal of LTB4-568 as a function of time at two different temperatures in the presence of BLT2-containing nanodiscs (○ and ●) or empty nanodiscs (□ and ■). (e) Binding of GTPγS to $G\alpha_i\beta\gamma$ catalyzed by empty or BLT2-containing nanodiscs in the absence of a ligand or in the presence of 1 μM LTB4 or LY255283. Data are presented as fluorescence intensities under a given condition (I) normalized to that measured under the same condition in the absence of any particle [$I(0)$]. (f) LTB4 or LY255283 saturation of binding of GTPγS to $G\alpha_{i2}\beta_1\gamma_2$ in the presence of BLT2-containing nanodiscs (○ and ●) or empty discs (□ and ■). The inset shows the time-dependent activation profiles. In all panels (a–f), data are represented as means ± the standard deviation of three representative experiments (**$p < 0.01$; ***$p < 0.001$).

tumbling complexes being studied in lipid-reconstituted integral membrane proteins.

To address all these issues, we devised an original strategy that associates overexpression in *Escherichia coli*, which allows the design of efficient isotope labeling schemes dedicated to the study of large protein complexes in solution by NMR, and subsequent reconstitution of the receptor in lipid nanodiscs.[18] This strategy was applied to a prototypical GPCR, the leukotriene B4 receptor BLT2. Because of perdeuteration of the receptor, we refined the current model of GPCR activation by providing evidence of multiple subconformations for transmembrane (TM) regions that are modulated by ligands and the lipid environment. As nanodiscs allow an analysis of the impact of lipids on receptor conformational dynamics, we focused here on the impact of the cholesterol analogue cholesteryl hemisuccinate (CHS). Indeed, most of the GPCRs are affected, at the functional and/or structural level, by the cholesterol content of their membrane environment.[19] In particular, adding cholesterol increased the activity of the other leukotriene B4 (LTB4) receptor, BLT1, which is closely related from a structural and functional point of view to BLT2 studied here.[20]

■ RESULTS AND DISCUSSION

Receptor Labeling and Functional Reconstitution in a Membrane Environment. To obtain the isotopically labeled BLT2 in nanodiscs, we devised a four-step method that is schematically presented in Figure S1. We selected a labeling scheme in which ^{12}C-labeled Met and Ile residues were perdeuterated and contained a protonated and ^{13}C-labeled methyl probe (for Ile, just the methyl at position δ_1 is ^{13}C-labeled and protonated). BLT2 contains only one isoleucine and five methionines. The position of these residues in the receptor structure was inferred from a homology model of BLT2 validated through NMR and site-directed mutagenesis[21] (Figure S2). Ile229$^{6.40}$ (Ballesteros–Weinstein indexing system in superscript) is located away from the putative ligand-binding site of BLT2 and is not directly involved in ligand binding.[21] Moreover, Ile229$^{6.40}$ is located close to the cytoplasmic part of the TM6 helix, a region that is considered to be most sensitive to GPCR activation.[22] Among the five methionines, only two (Met105$^{3.36}$ and Met197$^{5.54}$) belong to the TM part of the receptor; Met105$^{3.36}$ is located at the bottom of the ligand-binding pocket in TM3, and Met197$^{5.54}$ in TM5 is spatially close to Ile229$^{6.40}$ (Figure S2). The other Met residues are located either at the N-terminus or in the flexible C-terminal tail of the receptor. To focus only on conformational dynamics affecting the transmembrane domains and simplify the spectra, we mutated the N- and C-terminally located Met to Ala and considered only the transmembrane ones (Figure S3). The labeled receptor was then assembled into nanodiscs composed of partially deuterated dimyristoylphosphatidylcholine (DMPC) and protonated CHS as the lipids and stabilized by the protonated lipoprotein MSP1D1[18] (Figure S4). The use of DMPC was dictated by spectroscopic considerations, in particular by the fact that the deuterated version of this compound is easily available from commercial sources. Working with DMPC molecules in which both acyl chains

DOI: 10.1021/jacs.6b04432
J. Am. Chem. Soc. 2016, 138, 11170–11175

were perdeuterated allowed the acquisition of clean NMR spectra. As shown below, these lipids maintain the functional properties of the BLT2 receptor.

The reconstitution conditions used, i.e., large excess in lipoprotein, have been shown to systematically provide monomeric receptor preparations for all GPCRs considered so far (see Experimental Procedures in the Supporting Information). Use of a monomeric receptor, as we did here, simplifies the analysis, as dimeric assemblies are likely asymmetric in their conformational features.[23] Accordingly, the samples so obtained were homogeneous based on size-exclusion chromatography and negative-stained images obtained by electron microscopy (Figure S5). It is important that pharmacological characterization directly demonstrates that reconstitution of BLT2 in nanodiscs allows the receptor to adopt a native and stable conformation with regard to its ability to bind ligands and activate its cognate G protein partner under the conditions used in the NMR experiments (Figure 1). In particular, a molar binding ratio of 0.95 LTB4 per BLT2 was inferred from a stoichiometric titration assay in the absence of G protein (Figure 1a). If the 1:1 ligand:receptor stoichiometry we previously determined for binding of LTB4 to BLT2 is taken into account,[24] this means that 95% of the BLT2 receptors are ligand-competent in our preparations. Moreover, all dose-dependent ligand binding plots display a single class of binding sites, as expected for this receptor in the absence of G protein,[24] further demonstrating the homogeneity of our NMR sample (Figure 1).

Conformational Landscape of the Unliganded Receptor. NMR investigations of the BLT2 conformational landscape in a lipid bilayer environment were then conducted through acquisitions of two-dimensional (2D) $^{1}H-^{13}C$ correlation spectra. For these experiments, the labeled receptor in the unliganded state was assembled in nanodiscs with protonated lipoproteins at a low CHS concentration (0.03 CHS/DMPC molar ratio) in a 100% $^{2}H_2O$ Tris buffer solution. Under such conditions, the NMR experiments give rise to clean spectra with expected $^{13}CH_3$ correlation peaks belonging to either Met or Ile229$^{6.40}$ residues and essentially no residual natural abundance lipid signals from DMPC and CHS (Figure 2).

The position of a peak (^{1}H and ^{13}C chemical shifts) representing a methyl group in the NMR spectrum is dependent on the microenvironment of this methyl group in the protein. In proteins, the protons and carbon of these groups may experience a variety of environments that depend on both local and global protein structure. As a result, the position of the NMR peak is very sensitive to changes in protein conformation. The [δ_1-$^{13}CH_3$]-Ile229$^{6.40}$ group in the unliganded state of BLT2 displays four major peaks (Figure 2c), suggesting that it is detecting at least four distinct receptor conformational states in slow chemical exchange at 950 and 239 MHz (^{1}H and ^{13}C Larmor frequencies, respectively). It is important that these peaks likely not come from kinetically trapped states, as their intensity varied in the presence of BLT2-specific ligands (see below). In the same way, Met105$^{3.36}$ detects four different conformational states, as indicated by the occurrence of four cross-peaks for this residue (labeled A–D, Figure 2b). In contrast, Met197$^{5.54}$ displays a more restricted conformational space (Figure 2b), indicating that different domains of the receptor present different dynamic properties, as reported for other receptors, as well.[12] In the following, we will consider only Ile229$^{6.40}$, as Met105$^{3.36}$ essentially follows

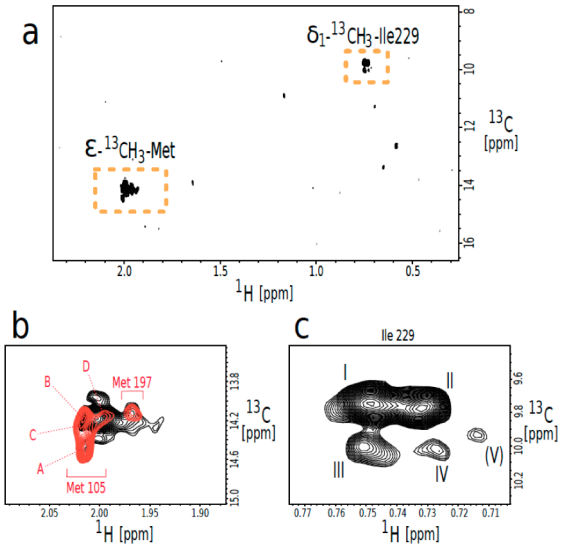

Figure 2. Conformational landscape of unliganded BLT2 in nanodiscs. 2D $^{1}H-^{13}C$ SOFAST-methyl-HMQC/TROSY spectrum acquired with [U-^{2}H,^{12}C]Ile-[δ_1-$^{13}CH_3$], [U-^{2}H,^{12}C]Met-[ε-$^{13}CH_3$] BLT2 in low-CHS content nanodiscs in the unliganded state. (a) Global view of the [ε-$^{13}CH_3$]-Met and [δ_1-$^{13}CH_3$]-Ile229$^{6.40}$ regions (boxed in orange); the additional weak peaks correspond to residual lipid signals. (b and c) From panel a, close-ups of the ε-$^{13}CH_3$-Met region and [δ_1-$^{13}CH_3$]-Ile229$^{6.40}$ region, respectively. In panel b, the red spectrum corresponds to that of a mutant receptor that contains the transmembrane Met residues 105$^{3.35}$ and 197$^{5.54}$ only. See Figure S6 for the assignments of Met105$^{3.35}$ and Met197$^{5.54}$. The peak labeled V in parentheses in panel c is not included in the present analysis of the BLT2 conformational ensemble [see also the spectrum in the presence of 12-HHT (Figure S8)]. Identical spectra were obtained from measurements with two independent samples.

the same trends that Ile229$^{6.40}$ does upon sterol content variation and ligand binding (Figure S6).

Peak intensity in 2D NMR spectra generally depends, in part, on the concentration of the observed state. Depending on the relaxation properties of each state and the experimental conditions, this intensity can be used to estimate relative populations. Altogether, states I, II, and III represent ~95% of the total [δ_1-$^{13}CH_3$]-Ile229$^{6.40}$ NMR signal in the unliganded state with a low CHS content (Table S1). These states are likely inactive conformations because we observed essentially no G protein activation under these conditions (Figure 3b). This suggests that BLT2 can adopt several alternative inactive states, as previously reported with β_2-adrenergic receptor (B2AR).[9,11]

The Receptor Conformational Landscape Is Modulated by a Sterol. In contrast to previous work in detergent solutions, the use of nanodiscs allows an analysis of the impact of membrane composition on receptor conformational exchange. In a first stage, we investigated the impact of sterols on this exchange. To this end, we performed NMR experiments with unliganded BLT2 assembled into nanodiscs at different CHS/DMPC molar ratios, i.e., low (0.03), intermediate (0.43), and high (0.98) ratios (Figure 3a), considering that usually the proportion of cholesterol is found to be 20–30 mol % in cell membranes, up to 50 mol % in red blood cells, and 70 mol % in the ocular lens membranes.[25] At the lowest CHS content, we expect the latter will first distribute within preferential sites and not in a random manner, based on the existence of cholesterol-binding sites on GPCRs.[26] CHS was used here instead of

DOI: 10.1021/jacs.6b04432
J. Am. Chem. Soc. 2016, 138, 11170–11175

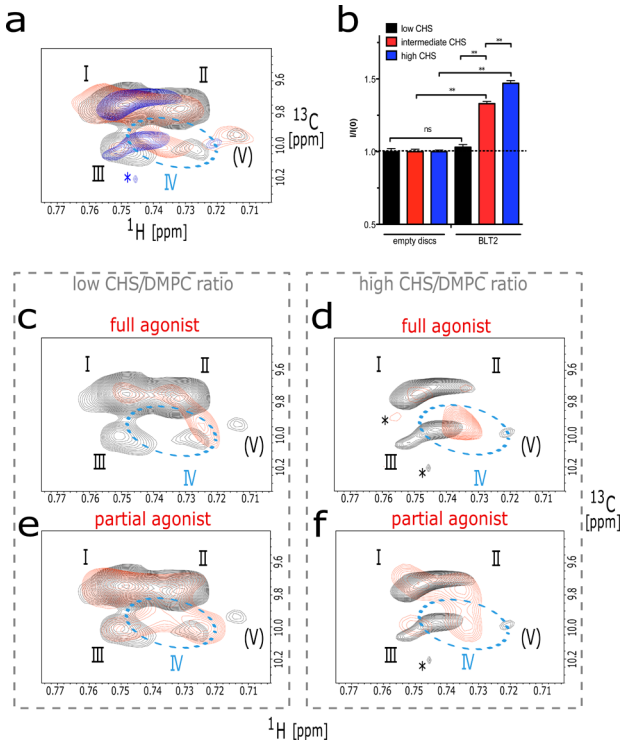

Figure 3. Impact of CHS content and ligands on the BLT2 conformational landscape and basal activity. (a) [δ_1-$^{13}CH_3$]-Ile229$^{6.40}$ region from 2D ^{1}H−^{13}C SOFAST-methyl-HMQC/TROSY superimposed spectra acquired at low (black), medium (red), and high (blue) CHS/DMPC ratios in the unliganded state. The dashed ellipse delineates the spectral region named state IV (reproduced in panels c−f), and the asterisk indicates some noise. (b) Binding of GTPγS to Gαi2 catalyzed by the BLT2 receptor in nanodiscs at low, intermediate, and high CHS contents in the absence of a ligand. Data are presented as fluorescence intensities under a given condition (I) normalized to that measured with empty nanodiscs under the same condition [$I(0)$]. Data are represented as means ± the standard deviation of three representative experiments (**p < 0.01; ***p < 0.001). (c−f) Close-ups of the [δ_1-$^{13}CH_3$]-Ile229$^{6.40}$ region of superimposed 2D NMR ^{1}H−^{13}C SOFAST-methyl-HMQC/TROSY spectra in the unliganded (black) and liganded (red) states at low (c and e) or high (d and f) CHS/DMPC ratios. Agonist and partial agonist refer to LTB4 and LY255283, respectively. In all cases, the dashed ellipse roughly delineates where state IV chemical shifts vary with changes in the CHS content of the nanodiscs. Identical spectra were obtained from measurements with two independent samples (see also Figure S9).

cholesterol, as its higher solubility in aqueous solutions was pivotal for strictly controlling its incorporation into nanodiscs (Figure S4). Moreover, this soluble analogue has been repeatedly used in studies aimed at delineating the role of cholesterol in GPCR structure and function.[27] The use of CHS as a cholesterol substitute was also further validated by a recent theoretical study.[28]

Cholesterol, or its slightly more soluble CHS analogue used in this study, is known to stiffen higher eukaryotic membranes by increasing the order of fatty acyl chains[25] (see also Figure S7). Increasing the CHS content from a CHS/DMPC molar ratio of 0.03 to 0.98 led to significant changes in the NMR spectrum (Figure 3a): the populations of states II and III substantially decreased in favor of states I and IV (Table S1). These changes in the NMR spectra were associated with changes in the functional properties of the receptor. Indeed, a significant increase in the extent of ligand-independent G protein activation was observed when the CHS content of the nanodiscs was increased (Figure 3b). The concomitant increase in state IV population and basal activity of BLT2 suggests that this state could correspond to an active/active-like conformation with regard to Gi activation, and that constitutive activity could be directly linked to the fraction of the receptor existing in state IV. Interestingly, our observation is in agreement with what has been reported for the closely related BLT1 receptor at the functional level, where removing membrane cholesterol attenuated responses to LTB4 whereas adding cholesterol enhanced this response.[20]

Cholesterol has been shown to affect GPCR functioning.[29,30] Our data directly support a model in which CHS has an impact on the conformational dynamics of the receptor. In the case of rhodopsin, it has been proposed that cholesterol affects the equilibrium between the active and inactive states via a combination of direct and indirect effects.[31] Indeed, in principle, cholesterol can bind directly to the protein[32] or indirectly affects the receptor by modifying the biophysical properties of the lipid bilayer.[33] At the present stage of the analysis, we cannot distinguish between the contributions of the two mechanisms to the reshaping of the BLT2 conformational landscape. In this context, it should be noted that the estimated phase transition temperature of deuterated DMPC in BLT2-containing nanodiscs is not significantly affected by variations in CHS content (Figure S7). Instead, CHS flattens the transition, suggesting a stiffening of the bilayer.

The Receptor Conformational Landscape Is Modulated by Ligands. To further assess how the conformational landscape of BLT2 is modulated, we conducted NMR experiments in the presence of ligands at low CHS contents. Only a limited number of ligands have been described for BLT2. Among them are the two natural agonists, LTB4 and 12-HHT.[34] However, 12-HHT is a heptadecanoid that is far less soluble than LTB4 and also binds to the empty discs (Figure S8). This precluded saturation of the ligand-binding site of BLT2 from being achieved at the protein concentration used in the NMR experiments, which in turn resulted in complex NMR spectra due to the occurrence of mixtures of ligand-free and 12-HHT-loaded BLT2 (Figure S8). In the presence of an excess of LTB4, the δ_1-Ile229$^{6.40}$ region of the spectrum displayed a more restricted conformational space as judged from the reduced number of cross-peaks (Figure 3c). In this case, state IV became the most populated state (Table S1), in addition to a slight variation in its NMR chemical shifts. These slight chemical shift variations occurred for state IV and were also observed in the unliganded state with the variation in CHS content. A tentative explanation would be to consider the fact that CHS stabilizes microconformations closely related to state IV. Another possibility would be that these slight changes reflect fast to intermediate time scale exchange between multiple states. In any case, the population of state IV thus significantly increases in the presence of the LTB4 agonist, in agreement with the assumption that state IV could correspond to an active or active-like conformation.

Besides the natural ligands LTB4 and 12-HHT, some synthetic compounds have been identified, among them LY255283 and ZK-158252. However, the latter antagonist displays a very low affinity for BLT2,[35] so that saturation of the ligand-binding site of the receptor could not be achieved in the receptor concentration range used in the NMR experiments. The analysis of the influence of synthetic ligands on the BLT2

DOI: 10.1021/jacs.6b04432
J. Am. Chem. Soc. 2016, 138, 11170−11175

conformational landscape was thus performed in the presence of LY255283. In this case, only a slight decrease in the complexity of the NMR spectra was observed (Figure 3e), and the moderate increase in the population of state IV was associated with a modest decrease in populations of states II and III (Table S1). The moderate increase in the population of state IV was fully consistent with the slight agonist activity of this compound in the BLT2-catalyzed GTPγS binding assay compared to LTB4 (Figure 1e,f). Interestingly, in this case, the population of the active-like conformation IV is intermediate between that in the absence of ligand and that in the presence of the full agonist LTB4. The differences in G protein signaling capacity could thus be due to the degree to which ligands shift the equilibrium toward state IV.

Allosteric Effects of CHS and Ligands on BLT2 Conformation. Because both CHS and the ligands affect the conformational landscape of BLT2, we finally analyzed whether they had additive effects on BLT2 conformation. At high CHS contents in the presence of either LTB4 or LY255283, the conformational space was more restricted than at low CHS contents (Figure 3d), with the occurrence of a very major species (state IV) that represented ∼80% of the total receptor population (Table S1). The presence of a high CHS content associated with that of the agonist thus leads to a restricted conformational space for BLT2 with a great predominance of its active-like state (Figure S9). These data therefore directly demonstrate an allosteric coupling between the lipids and the agonist that is likely important for the control of the signaling properties of GPCRs. Accordingly, increasing the CHS content increased the extent of receptor-catalyzed G protein activation in the presence of both ligands (Figure S10).

CONCLUSION

The receptor expression and labeling method we devised allowed high-resolution experimental NMR data to be obtained for a recombinant GPCR in nanodiscs. This opens new perspectives for detailed structural and dynamic investigations of unmodified GPCRs in a lipid bilayer, as illustrated here with BLT2. This is a major issue in the field, as illuminating the dynamic nature of these receptors should offer a key to understanding the fundamental molecular mechanisms governing signaling.

ASSOCIATED CONTENT

Supporting Information

The Supporting Information is available free of charge on the ACS Publications website at DOI: 10.1021/jacs.6b04432.

Detailed experimental procedures, pharmacological characterization of BLT2 in nanodiscs, NMR correlation peak volumes of $[\delta_1$-$^{13}CH_3]$-Ile$229^{6.40}$ signals, schematic description of the receptor preparation method, localization of the labeled residues, assignment of the two TM methionines, evaluation of the CHS/DMPC molar ratio of nanodiscs containing the BLT2 receptor, characterization of BLT2 in DMPC/CHS nanodiscs, impact of ligands on Met$105^{3.35}$ and Met$197^{5.54}$ residues at low CHS contents, transition phase temperature of deuterated DMPC in the BLT2-containing nanodiscs, NMR investigations of the BLT2 conformational landscape with the agonist 12-HHT, impact of CHS content and ligands on the BLT2 conformational landscape, and the effect of CHS on receptor-catalyzed G protein activation in the presence of ligands (PDF)

AUTHOR INFORMATION

Corresponding Authors

*laurent.catoire@ibpc.fr

*jean-louis.baneres@umontpellier.fr

Notes

The authors declare no competing financial interest.

ACKNOWLEDGMENTS

We thank Edith Godard, Christel Le Bon, and Fabrice Giusti (UMR 7099, IBPC) for technical assistance, Marie-Noëlle Rager and Sophie Walme (ChimieParisTech, Paris, France) for NMR control experiments with various lipids and detergents at 400 MHz, and Jérôme Boisbouvier (IBS, Grenoble, France) and Rime Kerfah (NMRBio) for advising on the use of $^{13}CH_3$-labeled precursors. Special thanks are due to Aurélie Di Cicco (Institut Curie) for technical assistance with the electron microscope and Audrey Solgadi (Faculté de Pharmacie-Université Paris-Sud) for mass spectrometry measurements. Jean-Luc Popot is gratefully acknowledged for a critical review of the manuscript. This work was supported by the CNRS, Paris Diderot University, and by grants Laboratoire d'Excellence (LabEx) DYNAMO and Equipements d'Excellence (EQUIPEX) CACSICE from the French Ministry of Research and from the French National Research Agency through the "Investments for the Future" (France-BioImaging, ANR-10-INSB-04) and generic (ANR-13-BSV8-0006) programs. Financial support from the Très Grandes Infrastructures de Recherche for NMR (TGIR-RMN-THC Fr3050 CNRS) for conducting the research is gratefully acknowledged. We also acknowledge the PICT-IBiSA Institut Curie (Paris, France).

REFERENCES

(1) Lagerstrom, M. C.; Schioth, H. B. *Nat. Rev. Drug Discovery* **2008**, *7*, 339.

(2) Luttrell, L. M.; Kenakin, T. P. *Methods Mol. Biol.* **2011**, *756*, 3.

(3) Mondal, S.; Khelashvili, G.; Johner, N.; Weinstein, H. *Adv. Exp. Med. Biol.* **2014**, *796*, 55.

(4) Mittermaier, A. K.; Kay, L. E. *Trends Biochem. Sci.* **2009**, *34*, 601.

(5) Sekhar, A.; Kay, L. E. *Proc. Natl. Acad. Sci. U. S. A.* **2013**, *110*, 12867.

(6) Bokoch, M. P.; Zou, Y.; Rasmussen, S. G.; Liu, C. W.; Nygaard, R.; Rosenbaum, D. M.; Fung, J. J.; Choi, H. J.; Thian, F. S.; Kobilka, T. S.; Puglisi, J. D.; Weis, W. I.; Pardo, L.; Prosser, R. S.; Mueller, L.; Kobilka, B. K. *Nature* **2010**, *463*, 108.

(7) Liu, J. J.; Horst, R.; Katritch, V.; Stevens, R. C.; Wuthrich, K. *Science* **2012**, *335*, 1106.

(8) Kofuku, Y.; Ueda, T.; Okude, J.; Shiraishi, Y.; Kondo, K.; Maeda, M.; Tsujishita, H.; Shimada, I. *Nat. Commun.* **2012**, *3*, 1045.

(9) Nygaard, R.; Zou, Y.; Dror, R. O.; Mildorf, T. J.; Arlow, D. H.; Manglik, A.; Pan, A. C.; Liu, C. W.; Fung, J. J.; Bokoch, M. P.; Thian, F. S.; Kobilka, T. S.; Shaw, D. E.; Mueller, L.; Prosser, R. S.; Kobilka, B. K. *Cell* **2013**, *152*, 532.

(10) Kim, T. H.; Chung, K. Y.; Manglik, A.; Hansen, A. L.; Dror, R. O.; Mildorf, T. J.; Shaw, D. E.; Kobilka, B. K.; Prosser, R. S. *J. Am. Chem. Soc.* **2013**, *135*, 9465.

(11) Manglik, A.; Kim, T. H.; Masureel, M.; Altenbach, C.; Yang, Z.; Hilger, D.; Lerch, M. T.; Kobilka, T. S.; Thian, F. S.; Hubbell, W. L.; Prosser, R. S.; Kobilka, B. K. *Cell* **2015**, *161*, 1101.

(12) Sounier, R.; Mas, C.; Steyaert, J.; Laeremans, T.; Manglik, A.; Huang, W.; Kobilka, B. K.; Demene, H.; Granier, S. *Nature* **2015**, *524*, 375.

DOI: 10.1021/jacs.6b04432
J. Am. Chem. Soc. 2016, 138, 11170−11175

(13) Kofuku, Y.; Ueda, T.; Okude, J.; Shiraishi, Y.; Kondo, K.; Mizumura, T.; Suzuki, S.; Shimada, I. *Angew. Chem., Int. Ed.* **2014**, *53*, 13376.
(14) Isogai, S.; Deupi, X.; Opitz, C.; Heydenreich, F. M.; Tsai, C. J.; Brueckner, F.; Schertler, G. F.; Veprintsev, D. B.; Grzesiek, S. *Nature* **2016**, *530*, 237.
(15) Popot, J. L. *Annu. Rev. Biochem.* **2010**, *79*, 737.
(16) Chung, K. Y.; Kim, T. H.; Manglik, A.; Alvares, R.; Kobilka, B. K.; Prosser, R. S. *J. Biol. Chem.* **2012**, *287*, 36305.
(17) Gautier, A.; Mott, H. R.; Bostock, M. J.; Kirkpatrick, J. P.; Nietlispach, D. *Nat. Struct. Mol. Biol.* **2010**, *17*, 768.
(18) Ritchie, T. K.; Grinkova, Y. V.; Bayburt, T. H.; Denisov, I. G.; Zolnerciks, J. K.; Atkins, W. M.; Sligar, S. G. *Methods Enzymol.* **2009**, *464*, 211.
(19) Pucadyil, T. J.; Chattopadhyay, A. *Prog. Lipid Res.* **2006**, *45*, 295.
(20) Sabirsh, A.; Bristulf, J.; Owman, C. *Eur. J. Pharmacol.* **2004**, *499*, 53.
(21) Catoire, L. J.; Damian, M.; Baaden, M.; Guittet, E.; Banères, J. L. *J. Biomol. NMR* **2011**, *50*, 191.
(22) Katritch, V.; Cherezov, V.; Stevens, R. C. *Annu. Rev. Pharmacol. Toxicol.* **2013**, *53*, 531.
(23) Damian, M.; Martin, A.; Mesnier, D.; Pin, J. P.; Banères, J. L. *EMBO J.* **2006**, *25*, 5693.
(24) Arcemisbehere, L.; Sen, T.; Boudier, L.; Balestre, M. N.; Gaibelet, G.; Detouillon, E.; Orcel, H.; Mendre, C.; Rahmeh, R.; Granier, S.; Vives, C.; Fieschi, F.; Damian, M.; Durroux, T.; Banères, J. L.; Mouillac, B. *J. Biol. Chem.* **2010**, *285*, 6337.
(25) Rog, T.; Pasenkiewicz-Gierula, M.; Vattulainen, I.; Karttunen, M. *Biochim. Biophys. Acta, Biomembr.* **2009**, *1788*, 97.
(26) Gimpl, G. *Chem. Phys. Lipids* **2016**, *199*, 61.
(27) Zocher, M.; Zhang, C.; Rasmussen, S. G.; Kobilka, B. K.; Muller, D. J. *Proc. Natl. Acad. Sci. U. S. A.* **2012**, *109*, E3463.
(28) Kulig, W.; Tynkkynen, J.; Javanainen, M.; Manna, M.; Rog, T.; Vattulainen, I.; Jungwirth, P. *J. Mol. Model.* **2014**, *20*, 2121.
(29) Chini, B.; Parenti, M. *J. Mol. Endocrinol.* **2004**, *32*, 325.
(30) Paila, Y. D.; Chattopadhyay, A. *Subcell. Biochem.* **2010**, *51*, 439.
(31) Soubias, O.; Gawrisch, K. *Biochim. Biophys. Acta, Biomembr.* **2012**, *1818*, 234.
(32) Lee, A. G. *Biochem. Soc. Trans.* **2011**, *39*, 761.
(33) Lundbaek, J. A.; Collingwood, S. A.; Ingolfsson, H. I.; Kapoor, R.; Andersen, O. S. *J. R. Soc., Interface* **2010**, *7*, 373.
(34) Okuno, T.; Iizuka, Y.; Okazaki, H.; Yokomizo, T.; Taguchi, R.; Shimizu, T. *J. Exp. Med.* **2008**, *205*, 759.
(35) Yokomizo, T.; Kato, K.; Hagiya, H.; Izumi, T.; Shimizu, T. *J. Biol. Chem.* **2001**, *276*, 12454.

DOI: 10.1021/jacs.6b04432
J. Am. Chem. Soc. 2016, 138, 11170−11175